

# On the SPH Approximations in Modeling Water Waves

**Kazimierz Szmidt**

Institute of Hydro-Engineering, Polish Academy of Sciences, ul. Kościarska 7, 80-328 Gdańsk, Poland,  
e-mail: jks@ibwpan.gda.pl

(Received March 28, 2013; revised November 24, 2013)

## Abstract

This paper presents an examination of approximation aspects of the Smoothed Particle Hydrodynamics (SPH) in modeling the water wave phenomenon. Close attention is paid on consistency of the SPH formulation and its relation with a correction technique applied to improve the method accuracy. The considerations are confined to flow fields within finite domains with a free surface and fixed solid boundaries with free slip boundary conditions. In spite of a wide application of the SPH method in fluid mechanics, the appropriate modeling of the boundaries is still not clear. For solid straight line boundaries, a natural way is to use additional (virtual, ghost) particles outside the boundary and take into account mirror reflection of associated field variables. Such a method leads to good results, except for a vicinity of solid horizontal bottoms where, because of the SPH approximations in the description of pressure, a stratification of the fluid material particles may occur. In order to illustrate the last phenomenon, some numerical tests have been made. These numerical experiments show that the solid fluid bottom attracts the material particles and thus, to prevent these particles from penetration into the bottom, a mutual exchange of positions of real and ghost particles has been used in a computation procedure.

**Key words:** water wave, SPH modeling, consistency, kernel correction

## 1. Introduction

The Smooth Particle Hydrodynamics (SPH) is a relatively new method, extensively used in solid and fluid mechanics. It is a purely Lagrangian mesh-free method in which the motion of a fluid is simulated by the motion of a number of material particles. Field variables of a problem, such as pressure, density, and momentum, are represented by point variables associated with each of the particles. The field variables are obtained from particle values, using interpolation functions known as kernels. The method aims at computing the distribution of these particles and the associated field variables at selected points in time. In order to describe the motion of these particles and their mutual interactions, Euler equations for the preservation of fluid continuity and momentum are applied. With respect to these equations, the SPH may be considered as a discrete solution for a distribution of material particles in the space domain, which is

arbitrary in principle. In accordance with such a discrete approach, the interpolation with a continuous kernel function is used to define derivative operators in the equations of the fluid motion. Although the fundamental equations of the SPH method have been derived on the assumption of the fluid's continuity, they serve equally well for problems in which discontinuities of field variables and the fragmentation of the fluid emerge. Examples of such cases are turbulent fluid motion and breaking water waves, in which the assumption of continuity is broken.

The literature on the subject is considerable. In the last two decades a number of papers have appeared in which different numerical solvers of the method have been developed and successfully applied to various problems of hydrodynamics. The fundamentals of the method are discussed in the important work of Monaghan (1992). The SPH theory and its application since its inception in 1977 may be found in Monaghan (2005), where a state of the art of the method is also given. A detailed discussion on the SPH formulation method may be found in Liu and Liu's monograph (2009), which also contains a vast bibliography on the subject. Particularly noteworthy among other contributions is the one by Colagrossi and Landrini (2003). These authors presented an implementation of the method to treat two-dimensional interfacial flows with different fluids separated by sharp interfaces. They also studied the classical dam-break problem including the two-phase approach. For irregularly scattered points, a re-initialization of a density field by means of a linear correction of a kernel function was used. More recently, Staroszczyk (2010) investigated the water flow generated by a dam break. As Colagrossi and Landrini (2003), he applied linearly corrected kernels to derive all equations of the SPH method (equations of the conservation of mass and momentum) at each level of the discrete time. In the above-mentioned papers, water is considered a slightly compressible fluid with an assumed pressure-density relation. With respect to the description of water gravity waves, in which water is commonly assumed as an incompressible fluid, attempts have also been made to formulate the SPH for incompressible flows. Incompressible fluid formulations may be found in the papers of Lo and Shao (2002) and Ataie-Ashtiani et al (2008). In these formulations, however, at each time step it is necessary to solve the Poisson equation for the fluid pressure, which increases computational time.

Along with a growing number of applications of the SPH to various problems in fluid mechanics, the problems of the stability and accuracy of the method have emerged, stimulating investigations on the consistency and completeness of the particle method. A general investigation methodology of the mesh-free methods, together with several suggestions for their improvement, is presented in Belytschko et al (1998). In particular, in order to restore the completeness of a kernel approximation, a correction transformation of such a kernel is proposed. The kernel correction method, as discussed in Belytschko et al (1998), is followed, among others, by Colagrossi and Landrini (2003), Dalrymple and Rogers (2006), and Staroszczyk (2010). In principle, such a modification of a standard kernel should improve the accuracy

of the SPH method. However, as pointed out by Liu and Liu (2006), such a kernel correction may lead to discrepancies in the description of field functions.

The present paper investigates the correction of standard kernels in the SPH approach in order to evaluate the usefulness of this modification. The main attention of this research is paid to the so-called reproducing conditions of the SPH formulation. The kernel correction, as described in the above-mentioned papers, is obtained from exact reproducing conditions, derived in this paper for an integral interpolation of a given function. The discrete particle formulation of these conditions does not lead to unique conclusions, and therefore great care must be taken in applying the kernel correction technique to describe the water wave phenomenon. The paper concludes with remarks on the formulation of boundary conditions at the solid boundaries of a fluid domain.

## 2. Fundamentals of the SPH Method

The SPH is an interpolation method based on the concept of integral representation of a function, say  $f(\mathbf{r})$ , by the following integral

$$\langle f(\mathbf{r}) \rangle = \int_S f(\mathbf{r}') W(|\mathbf{r} - \mathbf{r}'|, h) dS', \quad (1)$$

where  $S$  is the domain of integration, and  $W(|\mathbf{r} - \mathbf{r}'|, h)$  is the so-called smoothing function, or smoothing kernel function, or interpolating kernel, or simply kernel in the SPH literature. The parameter  $h$  in this equation is the smoothing length responsible for the shape of the kernel. The left-hand side of equation (1) is called the interpolant of  $f(\mathbf{r})$  (Monaghan 1992), since it is only a certain approximation of the original function. With respect to this approximation, in what follows, we omit the brackets on the left-hand side of the integral formula. If the kernel is the Dirac delta function  $\delta(\mathbf{r} - \mathbf{r}')$ , the equation defines the well known identity  $f(\mathbf{r}) = \int_S f(\mathbf{r}') \delta(\mathbf{r} - \mathbf{r}') dS'$ . The kernel  $W(\mathbf{r} - \mathbf{r}', h)$  in equation (1) is usually chosen to be an even function, which should satisfy a number of conditions. The first of them is the unity condition

$$\int_S W(\mathbf{r} - \mathbf{r}', h) dS' = 1, \quad (2)$$

The second is the delta function property

$$\lim_{h \rightarrow \infty} W(\mathbf{r} - \mathbf{r}', h) = \delta(\mathbf{r} - \mathbf{r}'). \quad (3)$$

For practical reasons, the kernel should also satisfy the compact condition

$$W(\mathbf{r} - \mathbf{r}', h) = 0 \quad \text{when} \quad |\mathbf{r} - \mathbf{r}'| > R, \quad (4)$$

where  $R$  is the radius of a circular support domain centred at  $\mathbf{r}$  for a two-dimensional case, or a spherical support domain in a three-dimensional case.

In addition to the above conditions, the kernel is assumed to be a non-negative function within the support domain. It is also desirable that this function decreases monotonically with the increasing distance from the field point  $\mathbf{r}$ . Finally, the kernel function should be continuous and sufficiently smooth to ensure an accurate approximation of a function and its space derivatives.

The literature on the subject suggests various forms of kernel functions with certain restrictions imposed on them to ensure desired properties, listed above. Frequently used are spline functions of a chosen order – for example, quadratic, cubic or quartic spline functions. Among others, a Gaussian function is of primary importance. For the two-dimensional case, the Gaussian kernel reads

$$W(r, h) = \frac{1}{\pi h^2} \exp(-q^2), \quad \text{where} \quad q = \frac{r}{h}, \quad r^2 = x^2 + y^2. \quad (5)$$

According to Monaghan (1992), it is always best to assume that the kernel is a Gaussian, and this is called the first golden rule of the SPH. With respect to this statement, further in this work we will only consider Gaussian kernels. In general, at points of the boundary of a finite support domain, the Gaussian kernel function is different from zero, and at the same time, the integral of the kernel over the support domain does not equal unity. Therefore, in order to overcome this inconsistency, it is reasonable to take into account the normalized kernel (Colagrossi, Landrini 2003)

$$W_N = \frac{[\exp(-q^2) - \exp(-R^2)]}{\int_S [\exp(-q^2) - \exp(-R^2)] dS'}, \quad R = \frac{\delta}{h}. \quad (6)$$

It can be demonstrated that this equation satisfies the unity condition (2). In numerical applications, the continuous integral interpolation is approximated by a discrete summation interpolation. In the discrete approach, the infinitesimal volume (surface)  $dS'$  in the integrand (1) is replaced by the finite volume  $V_b$  of the particle  $b$ . Thus, the elementary volume  $V_b$ , the density  $\rho_b$  and the mass of this particle  $m_b$  are related by

$$m_b = \rho_b V_b. \quad (7)$$

With respect to this formula, the continuous SPH representation for  $f(\mathbf{r})$  is substituted by the discrete particle approximation expressed in the following form

$$f(\mathbf{r}) = f(\mathbf{r})|_a = f_a = \sum_{b=1}^N \frac{m_b}{\rho_b} f(\mathbf{r}_b) W(\mathbf{r} - \mathbf{r}_b, h) \quad (8)$$

where  $b$  denotes the particle label, and the summation is taken over all particles in the finite support domain.

For example, the interpolation formula gives the following estimate for the density at the point  $\mathbf{r} = \mathbf{r}_a$

$$\rho_a = \sum_b \frac{m_b}{\rho_b} \rho_b W_{ab} = \sum_b m_b W_{ab}. \quad (9)$$

If  $h = \text{const}$ , then, from the last relation, it follows that

$$\int \rho_a d\tau = \sum_b m_b \int W_{ab} d\tau = \sum_b m_b = M \quad (10)$$

which shows that the mass is conserved exactly.

The essential feature of the discrete interpolant is that it enables us to construct a differentiable approximation of a function from its values at particle nodal points by means of the differentiable kernel. In the discrete approximation of fundamental equations of fluid dynamics one needs to construct approximations of the gradient and divergence differential operators. Following the interpolation mentioned above, such operators may be obtained by a direct differentiation of the kernel function. A more detailed discussion on differential operators with desired properties may be found in the papers by Monaghan (1992, 2005). To make further discussion clear, we attach here the interpolations of the gradient and divergence operators given in these papers. The interpolation of the gradient of a scalar function  $f$  at the particle  $a$  reads

$$\nabla f_a = \rho_a \sum_b m_b \left( \frac{f_a}{\rho_a^2} + \frac{f_b}{\rho_b^2} \right) \nabla_a W_{ab} \quad (11)$$

and the divergence of a vector field, say the velocity field  $\mathbf{v}$  at the particle  $a$ , can be found from

$$(\nabla \cdot \mathbf{v})_a = \frac{1}{\rho_a} \sum_b m_b (\mathbf{v}_b - \mathbf{v}_a) \cdot \nabla_a W_{ab}. \quad (12)$$

According to these results, one can derive the discrete interpolations of the continuity and momentum equations. For a slightly compressible fluid, one obtains

$$\left. \frac{d\rho}{dt} \right|_a = \sum_b m_b (\mathbf{v}_a - \mathbf{v}_b) \cdot \nabla_a W_{ab} \quad (13)$$

and

$$\left. \frac{d\mathbf{v}}{dt} \right|_a = - \sum_b m_b \left( \frac{\rho_a}{\rho_a^2} + \frac{\rho_b}{\rho_b^2} \right) \nabla_a W_{ab} + \mathbf{b}_a, \quad (14)$$

where  $\mathbf{b}$  denotes the gravity acceleration vector.

These equations are supplemented by an equation of state describing the pressure-density relation. In the SPH approach, equations (13) and (14) are integrated numerically in time with an assumed time step, dependent on the equation of state. For barotropic fluids, the use of the real bulk modulus in the equation of state would

result in extremely small time steps (Bonet and Lok 1999). Therefore, an artificial, smaller bulk modulus is used in such a way that a certain velocity (smaller than the sound speed) is taken into account instead of the sound speed. Frequently, the continuity and momentum equations are supplemented by the following equation of state (Monaghan 1992):

$$p(\rho) = P_0 \left[ \left( \frac{\rho}{\rho_0} \right)^\gamma - 1 \right]. \quad (15)$$

In this equation,  $P_0$  and  $\rho_0$  denote the reference pressure and density, and the parameter  $\gamma$  is usually taken as 7 for water and 1.4 for air (Colagrossi, Landrini 2003).

### 3. Reproducing Conditions

The discrete approximation presented above should represent as closely as possible the field functions of the problem considered. In order to assess the ability of the discrete approach to model field variables, it is reasonable to investigate reproducing conditions for the integral interpolation of a field function. For instance, in a discrete description of partial differential equations by means of the finite difference method (FDM), the concept of consistency has been introduced, which indicates how well the discrete method reproduces these differential equations. A finite difference scheme is consistent if it exactly represents the differential equations in the limit as the spacing of nodal points approaches zero (Liu, Liu 2009, Belytschko et al 1998). With respect to the SPH method, with an irregular distribution of nodal – particle points, it is difficult to estimate the consistency of this method, and therefore, reproducing conditions are examined instead. In the literature on the subject, the reproducing conditions emerge in the study of the stability and convergence of approximation schemes used for descriptions of functions and differential equations. In accordance with the SPH method, which operates on a countable set of points, the approximation consists in describing continuous field functions with acceptable accuracy by means of a set of approximating functions and information associated with these isolated particles.

In order to make further discussion clear, let us confine our attention to a problem two-dimensional in space (plane), with the Cartesian system of coordinate axes  $(x, y)$ . The integral interpolation formula (1) is written in the form

$$f(x, y) = \int_S f(x', y') W(|\mathbf{r} - \mathbf{r}'|, h) dS' = \int_S f(x', y') W dS', \quad (16)$$

where  $\mathbf{r} = (x, y)$ ,  $\mathbf{r}' = (x', y')$ , and  $dS' = dx' dy'$ .

Applying the Taylor series expansion procedure, one obtains

$$\begin{aligned} f(x', y') &= f(x, y) + f_{,x}(x' - x) + f_{,y}(y' - y) + \\ &+ \frac{1}{2} f_{,xx}(x' - x)^2 + f_{,xy}(x' - x)(y' - y) + \frac{1}{2} f_{,yy}(y' - y)^2 \end{aligned} \quad (17)$$

where terms up to the second order power have been taken into account.

In this equation, the lower indices denote the partial derivatives of the function with respect to the space coordinates. Substitution of this relation into equation (16) gives

$$\begin{aligned}
 f(\mathbf{r}) &= f(\mathbf{r}) \int_S W dS' + f_{,x}(\mathbf{r}) \int_S (x' - x) W dS' + f_{,y}(\mathbf{r}) \int_S (y' - y) W dS' + \\
 &+ \frac{1}{2} f_{,xx}(\mathbf{r}) \int_S (x' - x)^2 W dS' + f_{,xy}(\mathbf{r}) \int_S (x' - x)(y' - y) W dS' + \\
 &+ \frac{1}{2} f_{,yy}(\mathbf{r}) \int_S (y' - y)^2 W dS'
 \end{aligned} \tag{18}$$

From the comparison of the left- and right-hand sides of this equation, it follows that this relation is true if and only if the following conditions hold

$$\begin{aligned}
 M_0 &= \int_S W dS' = 1, \quad M_x = \int_S (x' - x) W dS' = 0, \\
 M_y &= \int_S (y' - y) W dS' = 0, \quad M_{xy} = \int_S (x' - x)(y' - y) W dS' = 0, \\
 M_{xx} &= \int_S (x' - x)^2 W dS' = 0, \quad M_{yy} = \int_S (y' - y)^2 W dS' = 0.
 \end{aligned} \tag{19}$$

These conditions are, by definition, weighted moments of the kernel support domain with respect to the Cartesian system of coordinate axes  $(x, y)$ . It can be seen that the two last conditions are not satisfied in general, i.e.  $M_{xx} \neq 0$  and  $M_{yy} \neq 0$ . This means, that for the symmetrical support domain (circular support domain of radius  $\delta > 0$ ) and the even kernel function satisfying unity condition, the interpolation (16) is exact only for linear (in our case bilinear) functions with disappearing second order derivatives over the support domain, i.e. for

$$f_{,xx}(\mathbf{r}) = 0, \quad f_{,yy}(\mathbf{r}) = 0 \quad \text{for } \mathbf{r} \in S. \tag{20}$$

A general form of a function, satisfying these conditions, may be expressed as

$$f(x, y) = \alpha_0 + \alpha_1 x + \alpha_2 y + \alpha_3 xy, \tag{21}$$

where  $\alpha_i$  ( $i = 0, 1, 2, 3$ ) are constants.

In particular, interpolation equation (1) reproduces exactly a linear function of the form

$$f(x, y) = \alpha_0 + \alpha_1 x + \alpha_2 y. \tag{22}$$

In a similar way, one may derive interpolation conditions for the space derivatives of a function. The integral approximation of the first derivative of the function  $f(x, y)$  can

be obtained by replacing the function  $f(x', y')$  in equation (18) by its derivative. On the other hand, this approximation may be derived by means of a direct differentiation of equation (18).

The conditions, presented above, have been derived for continuous fields and integral approximations of a given function. In order to transform them to a form appropriate for the discrete SPH method, the integration is substituted by the summation procedure with respect to a finite set of particles in the support domain of a particle or a space point (without a material particle) considered. Accordingly, the linear reproducing conditions described by the first three equations (19) are substituted by the following ones:

$$\begin{aligned} M_0^a &= \sum_b V_b W_{ab} = 1, & M_x^a &= \sum_b V_b (x_b - x_a) W_{ab} = 0, \\ M_y^a &= \sum_b V_b (y_b - y_a) W_{ab} = 0. \end{aligned} \quad (23)$$

where  $V_b = m_b/\rho_b$ .

These linear reproducing conditions are similar to those given by Belytschko et al (1998), which are derived by investigating a polynomial completeness of the approximation of a function by a finite set of approximating functions. With the latter approach, the approximation should reproduce the polynomial of the order  $k$  exactly if the approximation is complete to the order  $k$ . As in the case of equations (19) and (23), one may derive the reproducing conditions for the space derivatives of the linear field. Simple manipulations give

$$\begin{aligned} M_{x0}^a &= \sum_b V_b \frac{\partial W_{ab}}{\partial x_a} = 0, & M_{y0}^a &= \sum_b V_b \frac{\partial W_{ab}}{\partial y_a} = 0, \\ M_{x1}^a &= \sum_b V_b (x_b - x_a) \frac{\partial W_{ab}}{\partial x_a} = 1, & M_{y1}^a &= \sum_b V_b (y_b - y_a) \frac{\partial W_{ab}}{\partial y_a} = 1, \\ M_{x2}^a &= \sum_b V_b (y_b - y_a) \frac{\partial W_{ab}}{\partial x_a} = 0, & M_{y2}^a &= \sum_b V_b (x_b - x_a) \frac{\partial W_{ab}}{\partial y_a} = 0. \end{aligned} \quad (24)$$

As it has been mentioned above, for linear (bilinear) functions and integral interpolation with the kernel  $W$ , the relevant reproducing conditions in equations (18) are fulfilled identically. For the SPH particle approximations of linear functions, however, the associated conditions (23) are not satisfied in general. The last feature results from the approximation of integrals by the finite summation formulae, and, what is important, the summation over a support domain is usually carried out for irregularly distributed particles in this domain. Nevertheless, one can expect that for a sufficiently dense spacing of the particles in the support domain, the discrepancy in the fulfilment of these conditions will be negligibly small. On the other hand, the question arises as to the possibility of improving the SPH method for irregularly distributed material



particles. Several attempts, at improving the accuracy of this method have been reported in the literature. The simplest way may be to correct the density and velocity fields by means of an averaging procedure applied in numerical computations. By such a procedure, the distribution of these variables is smoothed over the problem domain. Other attempts can be found in Belytschko et al (1998), where a set of formulations is given which correct the SPH kernel functions, as well as their gradients. The latter correction technique is employed by Colagrossi and Landrini (2003) in the analysis of free surface and interface flow, and by Staroszczyk (2010) in his description of the free surface evolution, generated by a dam break. By means of such a procedure, in the first of these two papers a more regular pressure distribution is obtained with restored consistency of mass and density. The correction of the kernel function presented in the above-mentioned papers is based on the linear modification of the original kernel. Thus, the new kernel is written as

$$\widehat{W}_{ab} = [\alpha_0 + \alpha_1 (x_b - x_a) + \alpha_1 (y_b - y_a)] W_{ab}, \quad (25)$$

where  $\alpha_j$  ( $j = 0, 1, 2$ ) are constants for the considered point  $(x_a, y_a)$ .

In a similar way, the corrected components of the new kernel derivatives with respect to  $x$  and  $y$  coordinate axes are expressed in terms of the standard kernel function  $W_{ab}$  as follows:

$$\begin{aligned} \frac{\partial \widehat{W}_{ab}}{\partial x} &= [\beta_0 + \beta_1 (x_b - x_a) + \beta_2 (y_b - y_a)] W_{ab}, \\ \frac{\partial \widehat{W}_{ab}}{\partial y} &= [\gamma_0 + \gamma_1 (x_b - x_a) + \gamma_2 (y_b - y_a)] W_{ab}, \end{aligned} \quad (26)$$

where  $\beta_j$   $\gamma_j$  ( $j = 0, 1, 2$ ) are constants.

From substitution of equation (25) into the linear reproducing conditions (23), the following system of equations is obtained:

$$[\mathbf{A}](\alpha) = (PA), \quad (27)$$

where

$$[\mathbf{A}] = \left\{ \sum_b V_b W_{ab} \begin{bmatrix} 1 & (x_b - x_a) & (y_b - y_a) \\ (x_b - x_a) & (x_b - x_a)^2 & (x_b - x_a)(y_b - y_a) \\ (y_b - y_a) & (y_b - y_a)(x_b - x_a) & (y_b - y_a)^2 \end{bmatrix} \right\} \quad (28)$$

and

$$(\alpha)^T = (\alpha_0 \ \alpha_1 \ \alpha_2) \quad \text{and} \quad (PA) = (1 \ 0 \ 0). \quad (29)$$

Substitution of (26) into the reproducing conditions (24) gives a system of equations, similar to (27), with the same matrix  $[\mathbf{A}]$  and the associated vectors

$$\begin{aligned} (\beta)^T &= (\beta_0 \ \beta_1 \ \beta_2) \quad \text{and} \quad (PB) = (0 \ 1 \ 0), \\ (\gamma)^T &= (\gamma_0 \ \gamma_1 \ \gamma_2) \quad \text{and} \quad (PC) = (0 \ 0 \ 1). \end{aligned} \quad (30)$$

The solution of equations (27) is written in the form

$$(\alpha) = [\mathbf{A}]^{-1}(PA) = [\mathbf{C}](PA). \quad (31)$$

The solution of the remainder equations for  $(\beta)$  and  $(\gamma)$  is defined by the same matrix  $[\mathbf{C}]$  and the associated vectors  $(PB)$  and  $(PC)$ , respectively. Thus, for the derivation of the corrected kernel and its derivatives at a given point, it is sufficient to calculate the inverse of the matrix  $[\mathbf{A}]$  and then products of the inverse with the relevant vectors, forming the unit diagonal matrix. From the comparison of equations (27) and (32) with the reproducing integral conditions, given in (19), some conclusions may be drawn. First, for an isotropic case and symmetrical kernels, all components of the matrix  $[\mathbf{A}]$ , except for those on the main diagonal, should be equal (or close) to zero. For such a case,  $\alpha_0 \cong 1$ ,  $\alpha_1 \cong \alpha_2 \cong 0$ , and the corrected kernel is equal to the original one. Second, for the case of an irregular distribution of particles, one may expect another, in general non-zero, solution of equation (27). It should be noted that in the latter case, the desired properties of the kernel function, described in Section 2 of this paper, are lost. With such a transformation, it may happen that the matrix  $[\mathbf{A}]$  becomes a singular matrix, which can lead to the breakdown of computations. Moreover, the new kernel may lead to unphysical representations of the field variables, such as negative density or negative energy (see Liu, Liu 2009). In particular, it is not possible to control the main features of the correction and its accuracy during the computation process. Summing up, special care must be taken in applying the method to hydrodynamic problems, and therefore, the kernel correction method is not recommended for the analysis of the water wave phenomenon.

#### 4. Boundary Conditions

In applying the SPH method to water wave mechanics, the problem of a particle formulation of boundary conditions at the fluid boundary emerges. Since the method applies to a collection of material particles moving in space, the fluid boundary is defined as a set of conditions imposed on particles reaching points at this boundary. It is relatively simple to describe the free surface of the fluid, which, in the material description employed in the SPH approach, is defined by the positions of material particles forming this surface. It should be stressed, however, that only particles at or near the boundary contribute to the summation of particle interactions. With respect to these particles, their finite supports are usually truncated by this boundary, and thus some discrepancies in calculating the pressure and the fluid density may occur. Even more serious problems arise in the formulation of the SPH boundary conditions at solid, fixed or moving, boundaries of the fluid domain. For a solid (rigid), free-slip boundary, the normal component of the velocity field should be equal to zero. An example of such a boundary is the case of a straight line solid boundary, usually found in the analysis of gravitational waves propagating in water of finite depth, as illustrated in Fig. 1. In order to solve this boundary condition, virtual particles are placed outside

the fluid domain, as marked in this figure. Such a model of a solving the boundary condition with additional mirror particles is used by Lo and Shao (2002) in simulating near-shore solitary wave mechanics and by Staroszczyk (2010) in simulating water flow generated by a dam break. The additional particles in the figure have the same density and pressure as the particles on the other side of the boundary, but the perpendicular component of their velocity has the opposite sign. In the case shown in Fig. 1, the use of the mirror particles corresponds directly to the solution of a symmetrical problem in a continuum in which the bottom line is the symmetry line of the problem domain considered. With respect to this problem, however, in the SPH approach, these virtual, additional particles are distributed within a strip of finite width  $\delta$ , which equals the assumed radius of a typical support domain. The problem becomes more complicated in the case of a boundary formed by a set of segments intersecting at corner points, or in the case of a curved boundary. If the segments intersect at right angles, the best solution is to use the mirror reflection of material particles within a strip along the boundary. In the case of an arbitrary angle of intersection, or in the case of a curved boundary, however, it is not possible to find a unique distribution of virtual (additional) particles to solve boundary conditions.

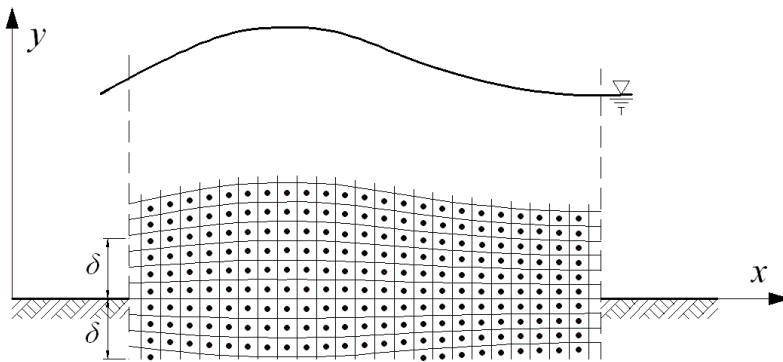


**Fig. 1.** Straight line solid boundary with fluid and virtual particles

The SPH equations are usually written for particles inside the fluid domain. Therefore, for the inner particles placed near the boundary, the contribution of virtual particles in the interpolation over the support domain is necessarily less than that of the inner particles (the contribution is the same only for particles at the boundary). This means that, in the SPH model, the phenomenon of attraction of fluid particles by solid boundaries may occur. Such attraction is induced by forces resulting from non-equal contributions of pressure gradients, which act on material particles near the boundary. In the literature on the subject, several attempts have been made to prevent the inner fluid particles from accumulating in the vicinity of solid boundaries. Usually, additional boundary particles are employed to generate repulsive forces on fluid particles (Morris et al 1997, Monaghan 2005, Ataie-Ashtiani et al 2008, Monaghan and Kajtar

2009). These repulsive forces prevent the real particles from penetrating the boundary. A way to specify the forces is to use a Lenard-Jones force acting between the centers of the particles (Monaghan 2005). On the other hand, such forces, acting on particles moving parallel to the boundary may cause large disturbances to flow near the boundary. In fact, such repulsive forces do not result from a solution in fluid dynamics, and therefore they should be employed with great care. As far as curved boundaries are concerned, a special boundary treatment is described by Liu and Liu (2009), who, in addition to real particles within a circular fluid domain, use virtual boundary (type I) particles and exterior (type II) particles to solve the boundary conditions at the domain circumference. Despite the several attempts mentioned above, the problem of a proper formulation of boundary conditions in the SPH method is still open. In the following, an approximate solution of boundary conditions at a curved boundary is presented, which may also be used for boundaries formed by intersecting straight segments. The normal components of the fluid velocity at boundary points should be equal to zero. In our approach, this boundary is represented by a number of segments of constant length. Outside the fluid, along this boundary, a set of virtual particles is added with mass, density and velocity components tangent to the boundary, which are equal to their counterparts in the fluid domain. The normal components of the velocity of these virtual particles are not known at this moment. The problem is linear, and therefore these velocity components can be chosen in such a way that the normal components of the velocity at selected boundary points disappear. Thus, for a typical boundary point, say  $r$  ( $r = 1, 2, \dots, n$ ), where  $n$  denotes the number of segments forming the boundary, the normal velocity is described by the formula

$$V_r = \sum_{b=1}^K \frac{m_b}{\rho_b} V_N^b W_{rb} + \sum_{k=r-p}^{k=r+p} \frac{m_k}{\rho_k} X_N W_{rk} = 0, \quad (32)$$

where  $V_N^b$  denote the projection of fluid particle velocities and the tangent velocity components of the virtual particles on the normal direction to the boundary at the boundary point  $r$ ,  $X_N$  are the unknown normal velocities of the virtual particles, and  $2p$  is the number of virtual particles within the support of the point  $r$ . The second part of the right-hand side of this equation denotes the contribution of the unknown normal components of the virtual particles. Equations (32) are written for all points of the boundary. The system of equations obtained in this way enables us to calculate the normal components of the velocity of the virtual particles. It should be stressed, however, that the accuracy of the formulation depends on the number of particles within the support domain for each point of the boundary, and therefore one must expect a relative discrepancy in the solution accuracy in the vicinity of corner points. The solution to the boundary conditions presented above requires additional computations, and thus it may be cumbersome to apply, especially for a complicated geometry

of the boundary. In order to estimate the efficiency of the formulation, some numerical tests are presented in the next section.

## 5. Numerical Experiments

In order to illustrate the discussion presented in the preceding sections, in what follows we will consider some numerical experiments for a fluid flow in a plane, rectangular basin of water, as shown schematically in Fig. 2. A non-viscous incompressible fluid is assumed to be a seiche water flow, i.e. a periodic motion with the angular frequency  $\omega$ , corresponding to a standing water wave of the length  $\lambda = 2L$ , where  $L$  is the length of the fluid domain. In the SPH formulation, a finite number of material particles is substituted for the fluid domain. The discrete solution of the problem is reduced to the integration in time of the continuity and momentum equations written for all particles. For each particle, we have the following system of differential equations:

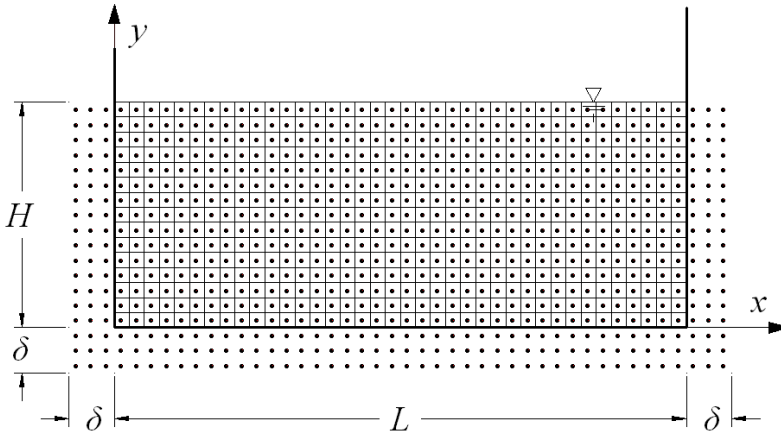


**Fig. 2.** Plane rectangular basin of water with vertical and horizontal solid boundaries

$$\frac{d\rho_a}{dt} = M_a, \quad \frac{d\mathbf{v}_a}{dt} = \mathbf{F}_a, \quad \frac{d\mathbf{x}_a}{dt} = \mathbf{G}_a \quad (33)$$

where

$$M_a = \sum_b m_b (\mathbf{v}_a - \mathbf{v}_b) \nabla_a W_{ab} \quad (34)$$

and

$$\mathbf{F}_a = - \sum_b m_b \left( \frac{p_a}{\rho_a^2} + \frac{p_b}{\rho_b^2} \right) \nabla_a W_{ab} + \mathbf{b}_a. \quad (35)$$

In this equation,  $\mathbf{b}_a = (0, -g)$  denotes the gravity acceleration vector. The term  $\mathbf{G}_a$  in the third equation in (33) denotes a corrected velocity of the particle  $a$ . The velocity correction is assumed in the form proposed by Monaghan (1992)

$$\mathbf{G}_a = \mathbf{v}_a + \sum_b \frac{m_a}{\rho_a + \rho_b} (\mathbf{v}_b - \mathbf{v}_a) W_{ab}, \quad (36)$$

which aims at smoothing the velocity of a given particle.

For consistency, the corrected velocities are also used in equation (34). A similar correction is performed for the density field at selected points in time by means of the formula

$$\rho_a = \sum_b m_b W_{ab} \quad (37)$$

The evolution equations (33) are integrated numerically in a discrete time domain by applying an explicit two-step predictor-corrector scheme. Thus, in the first step, the mid-step values of the particle's density, velocity and position are calculated

$$\rho_a^{k+1/2} = \rho_a^k + \frac{\Delta t}{2} M_a^k, \quad \mathbf{v}_a^{k+1/2} = \mathbf{v}_a^k + \frac{\Delta t}{2} \mathbf{F}_a^k, \quad \mathbf{x}_a^{k+1/2} = \mathbf{x}_a^k + \frac{\Delta t}{2} \mathbf{G}_a^k \quad (38)$$

where  $\Delta t = t^{k+1} - t^k$  is the time step length.

Then, in the second, final step, the values of the dependent variables are calculated according to the formulae

$$\rho_a^{k+1} = \rho_a^k + \Delta t M_a^{k+1/2}, \quad \mathbf{v}_a^{k+1} = \mathbf{v}_a^k + \Delta t \mathbf{F}_a^{k+1/2}, \quad \mathbf{x}_a^{k+1} = \mathbf{x}_a^k + \Delta t \mathbf{G}_a^{k+1/2}. \quad (39)$$

In order to ensure the stability of the numerical integration, the time step  $\Delta t$  should satisfy the so-called CFL condition that the speed of the initial particle spacing be greater than the reference speed (in our case the reference speed is smaller than the sound speed) (Toro 1997).

To complete the integration procedure, it is necessary to formulate initial conditions. For the present problem of a periodic fluid motion in a rectangular fluid domain, an analytical solution for a potential motion of a non-viscous incompressible fluid is employed. For the case shown in Fig. 2, the velocity potential is written in the form

$$\phi(x, z, t) = \frac{Ag}{\omega} \frac{\cosh(kz)}{\cosh(kH)} \cos(kx) \cos(\omega t) \quad (40)$$

where  $A$  is a constant, and  $k = \pi/L$  is the wave number with the following dispersion relation:

$$\omega^2 = gk \tanh(kH). \quad (41)$$

Following the potential function, one may calculate the free surface elevation

$$\eta(x, t) = A \cos(kx) \sin(\omega t), \quad (42)$$

the velocity components

$$\begin{aligned} u &= \frac{\partial \phi}{\partial x} = -\frac{Agk}{\omega} \frac{\cosh(kz)}{\cosh(kH)} \sin(kx) \cos(\omega t), \\ v &= \frac{\partial \phi}{\partial z} = \frac{Agk}{\omega} \frac{\sinh(kz)}{\cosh(kH)} \cos(kx) \cos(\omega t), \end{aligned} \quad (43)$$

and the relevant fluid pressure

$$p = \rho g(H - z) + A\rho g \left( \frac{\cosh(kz)}{\cosh(kH)} - 1 \right) \cos(kx) \sin(\omega t). \quad (44)$$

The formulae written above were used to describe the initial conditions at  $t = 0$ . With respect to the rectangular fluid domain at  $t = 0$ , the uniform spacing  $ax = az$  of material particles with the same initial density  $\rho_0$  was chosen to represent the fluid domain in the SPH formulation. In order to calculate the evolution in time of the field functions of the problem considered, equations (38) and (39) were applied for the discrete integration in the time domain with the constant time step  $\Delta t = 2 \times 10^{-4}$  s. To save computation time, a relatively small rectangular fluid domain with the initial height  $H = 0.20$  m and the length  $L = H$  was considered. Three grid resolutions were applied: the first with the initial inter-particle spacing  $d = ax = 0.02$  m, the second in which  $d = 0.01$  m, and the third with the  $d = 0.005$  m. The numbers of particles were  $N = 100$  for the first spacing,  $N = 400$  for the second, and  $N = 1600$  for the third. Numerical experiments, conducted for the three radii of the support domain, i.e. for  $\delta = 3d$ ,  $4d$  and  $5d$ , show that sufficiently good results were obtained for  $\delta = 4d$ , and therefore only that radius was selected for our computations. The smoothing length  $h$ , used in the kernel function (6), was chosen to be equal to  $4d/3$ , and the physical parameters appearing in the pressure equation (17) were  $P_0 = 10^5$  Pa and  $\rho_0 = 10^3$  kg/m<sup>3</sup>. At the fluid-solid boundaries (two vertical walls and the horizontal bottom, shown in Fig. 2) free-slip conditions were applied. In the discrete model considered, these conditions were implemented by means of additional (virtual) particles placed outside the boundaries, as illustrated in Fig. 2. The parameters of these virtual particles were chosen from the mirror reflection of the parameters associated with their counterparts within the fluid domain. The width of the virtual particle strip was equal to the radius of a typical support domain of a fluid particle. For comparison, the solution to boundary conditions was also constructed with the help of a single strip of virtual particles placed along the boundaries and with the application of conditions expressed by equations (32).

In the first step, the standard Gaussian and corrected kernel functions were used in the numerical procedure to assess the usefulness of the kernel correction, as discussed in the preceding sections. In numerical calculations, the constant number of  $N = 400$  particles was chosen to represent the fluid domain. Some computation results are presented in Fig. 3, in which the graphs show the distribution of the material

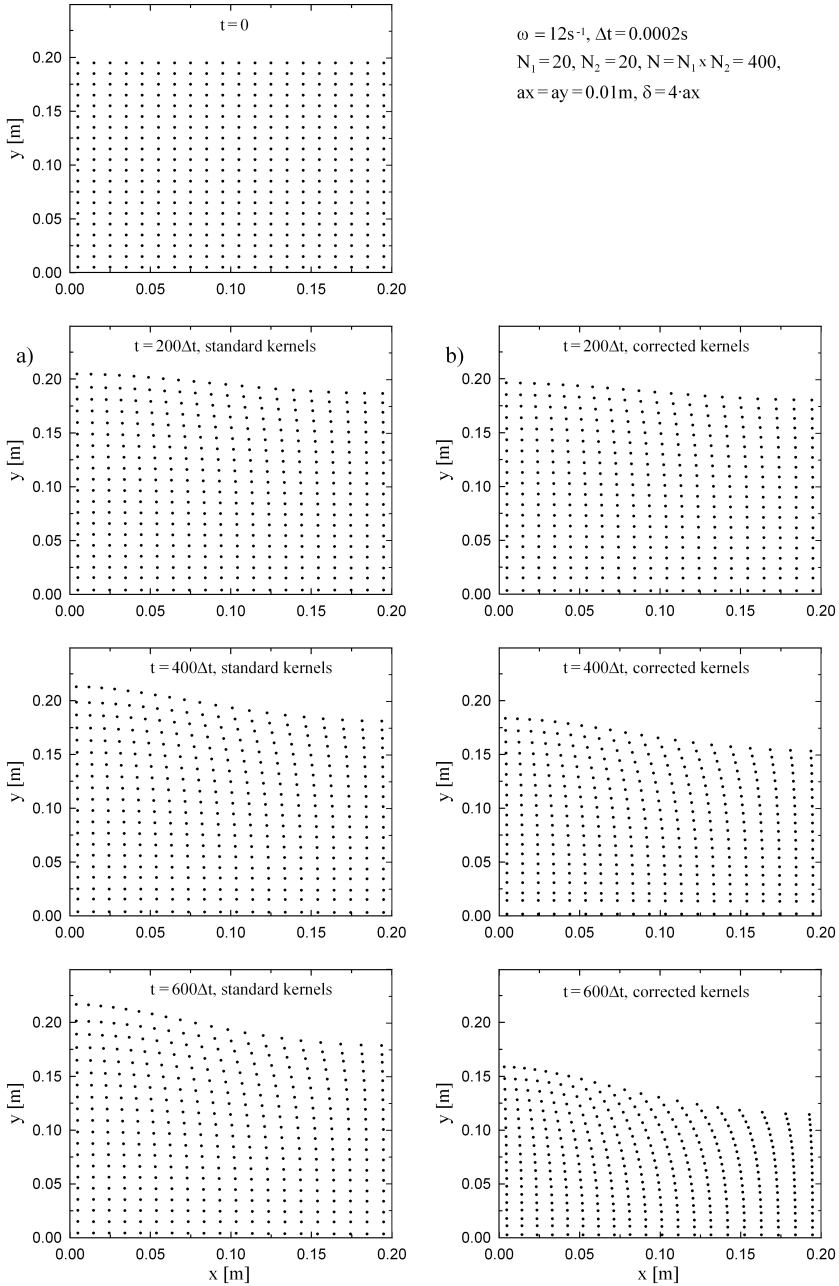


**Fig. 3.** Distributions of fluid particles at selected points in time: (a) calculated with standard kernels and (b) corresponding to corrected kernels



$$\omega = 12\text{s}^{-1}, \Delta t = 0.0002\text{s}, L = 0.20\text{m}, H = 0.20\text{m}, \delta = 4 \cdot ax$$

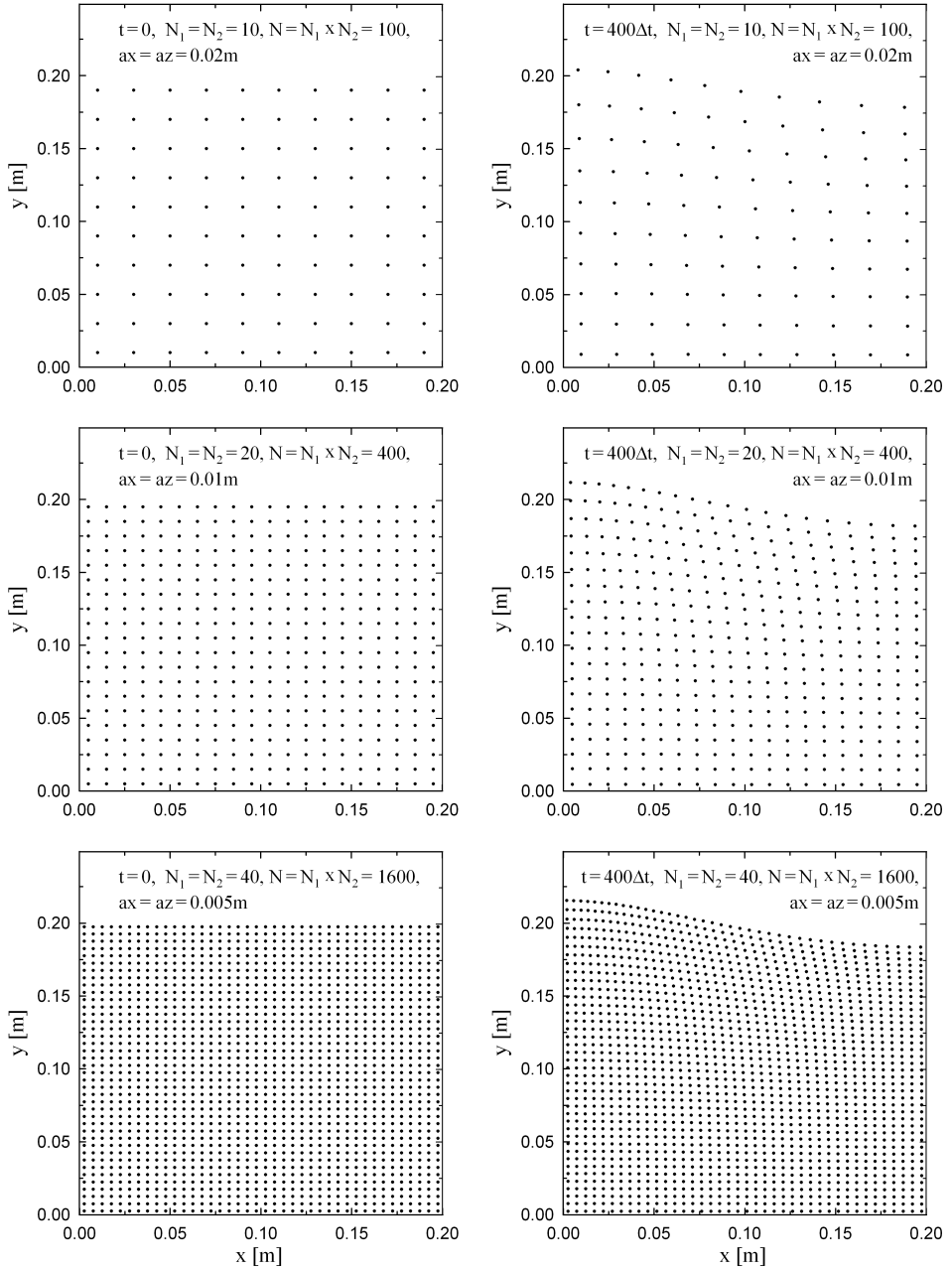


**Fig. 4.** Distributions of fluid particles at selected points in time, obtained for the three radii of the support domain

$$\omega = 12\text{s}^{-1}, \Delta t = 0.0002\text{s}, L = 0.20\text{m}, H = 0.20\text{m}, \delta = 4 \cdot ax$$

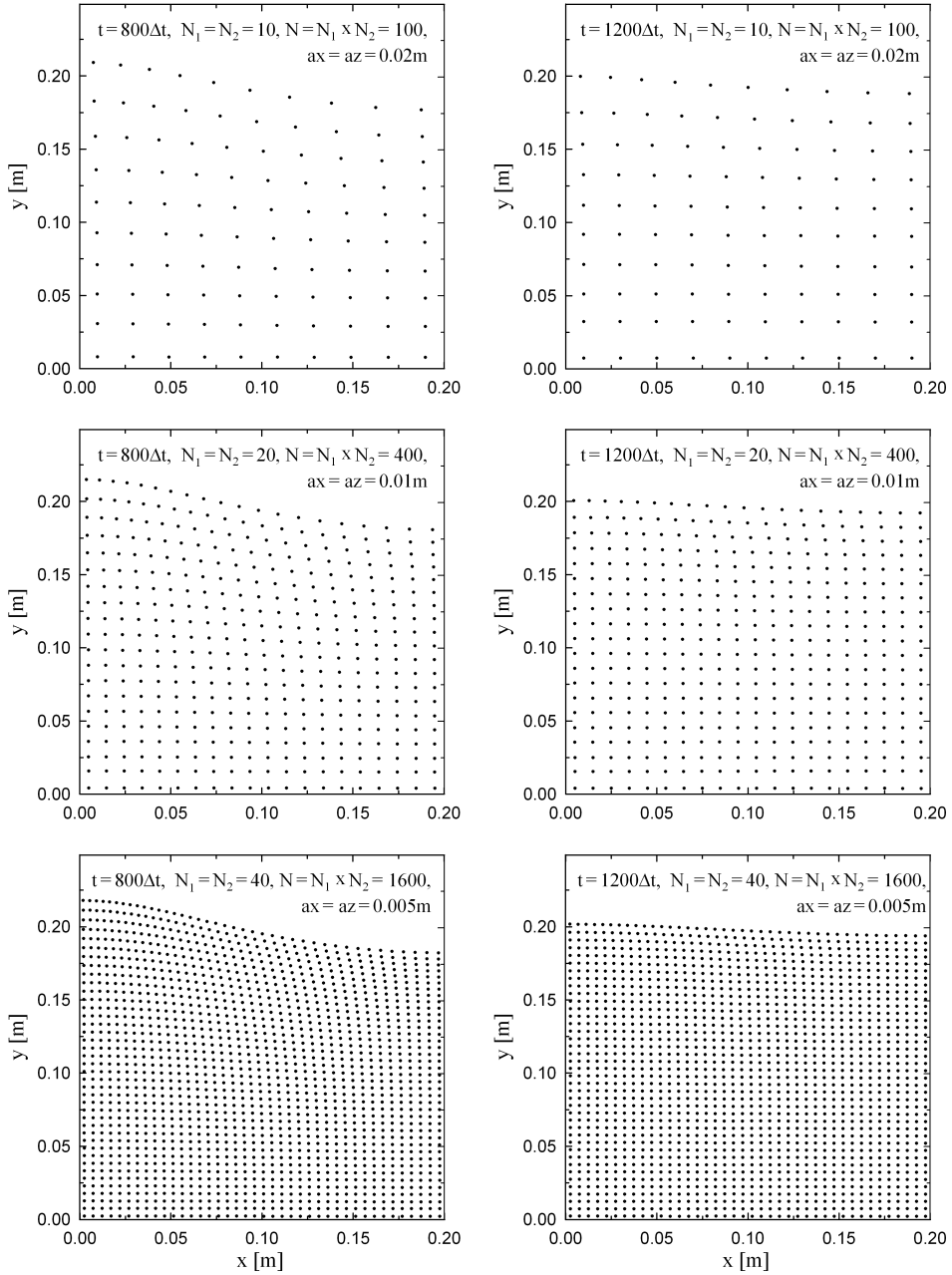


**Fig. 4.** Continued

$$\omega = 12\text{s}^{-1}, \Delta t = 0.0002\text{s}, L = 0.20\text{m}, H = 0.20\text{m}, \delta = 4 \cdot ax$$

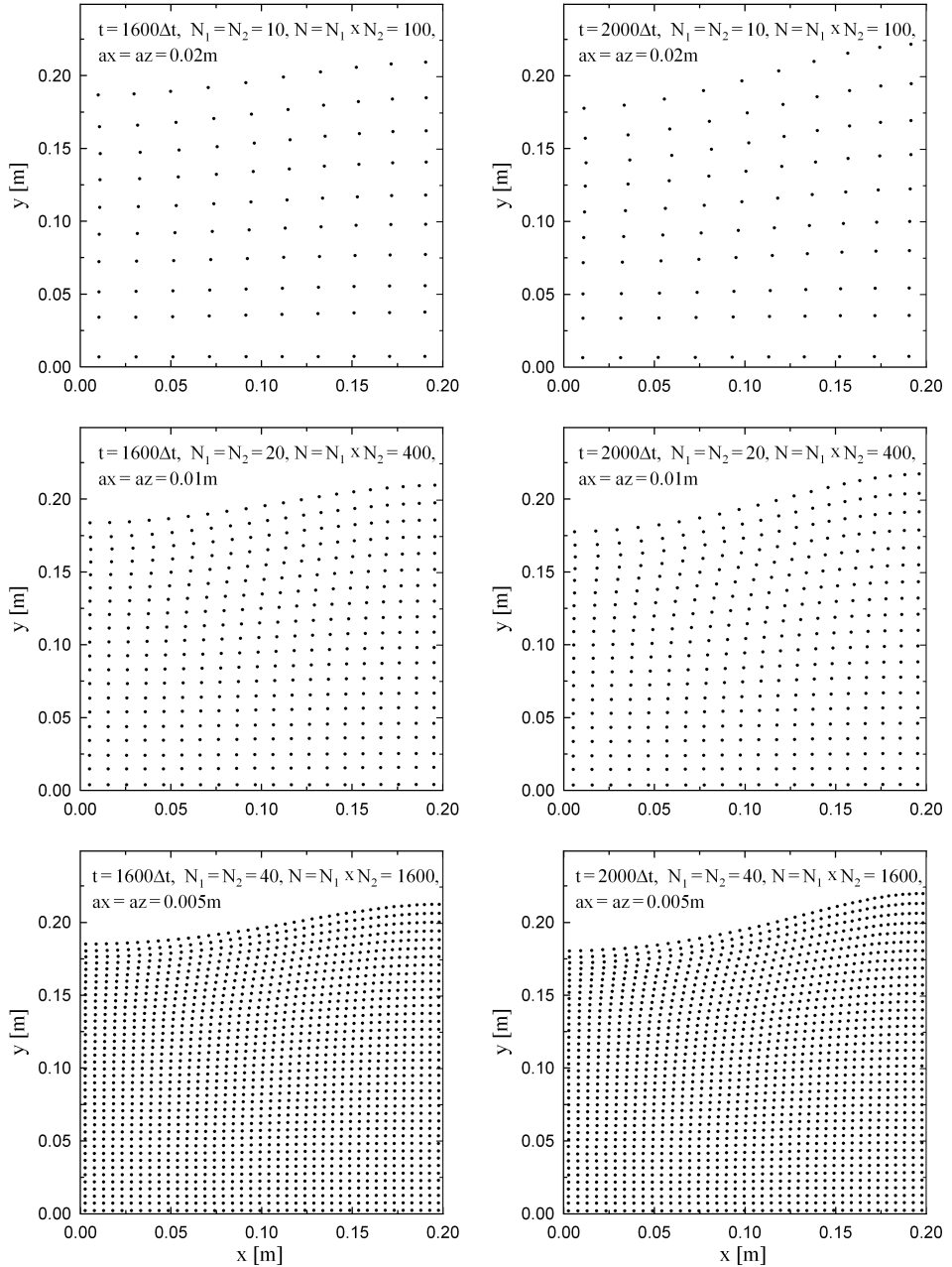


**Fig. 4.** Continued

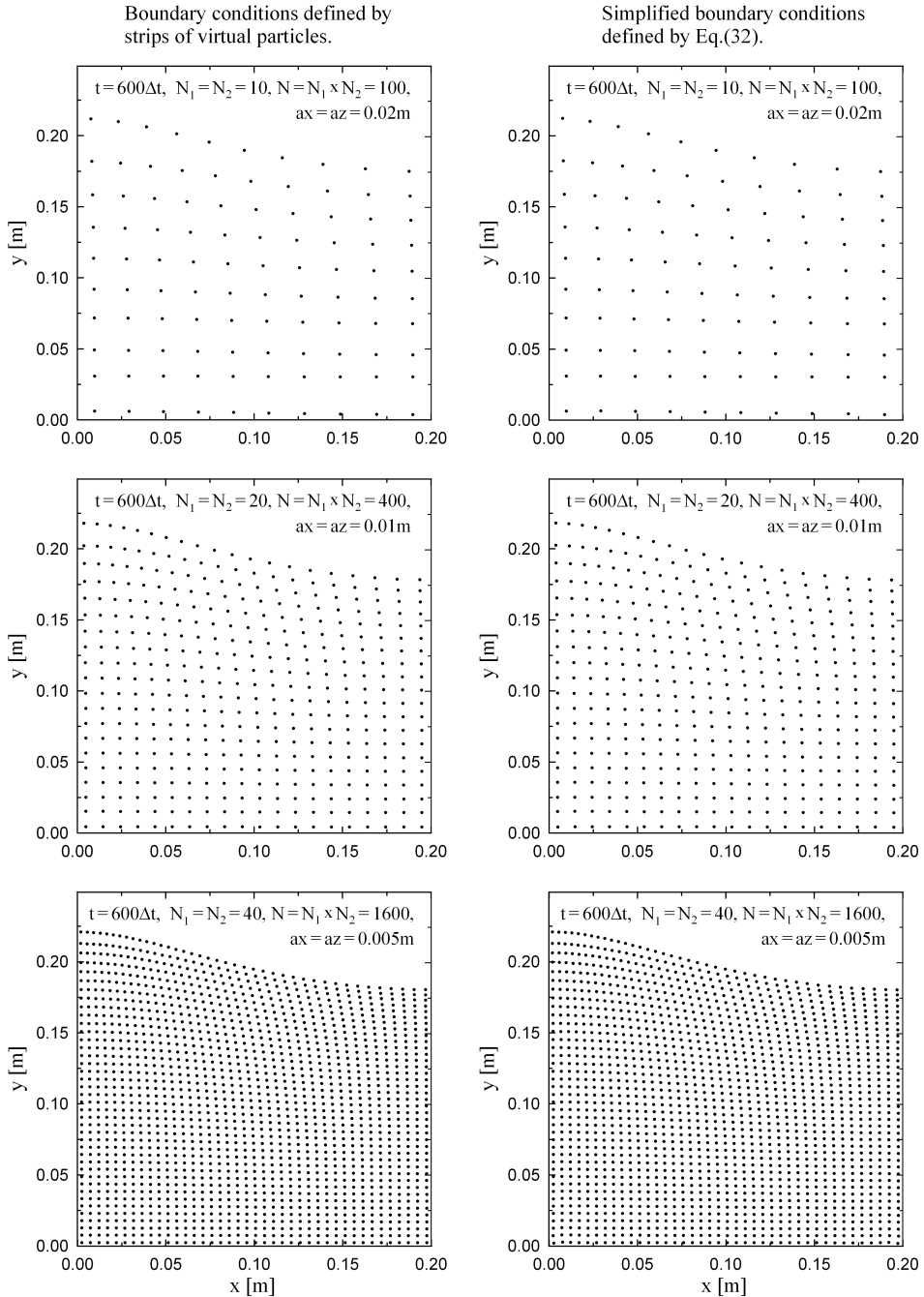


**Fig. 5.** Distributions of fluid particles at selected points in time, calculated for different formulations of boundary conditions

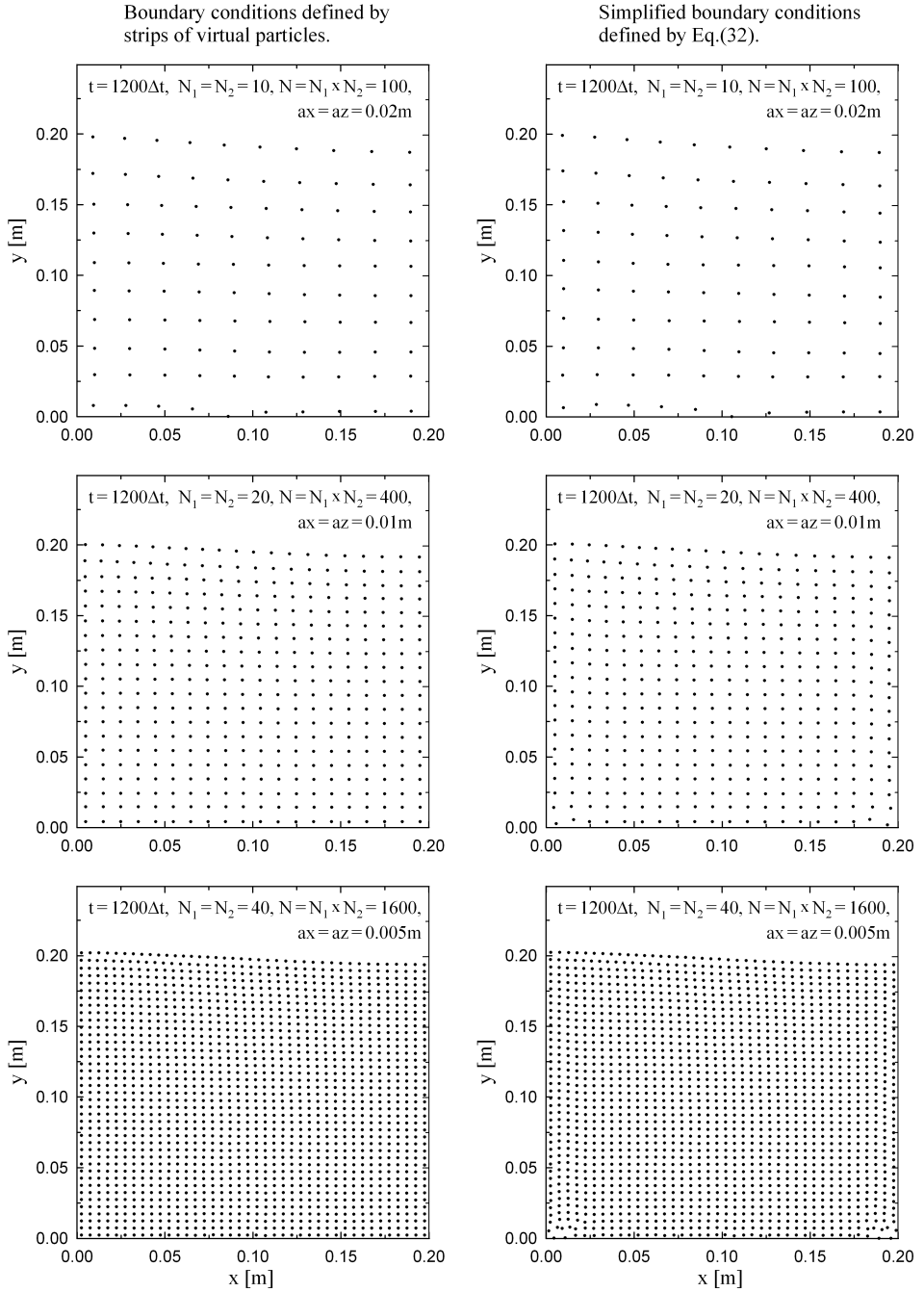


Fig. 5. Continued

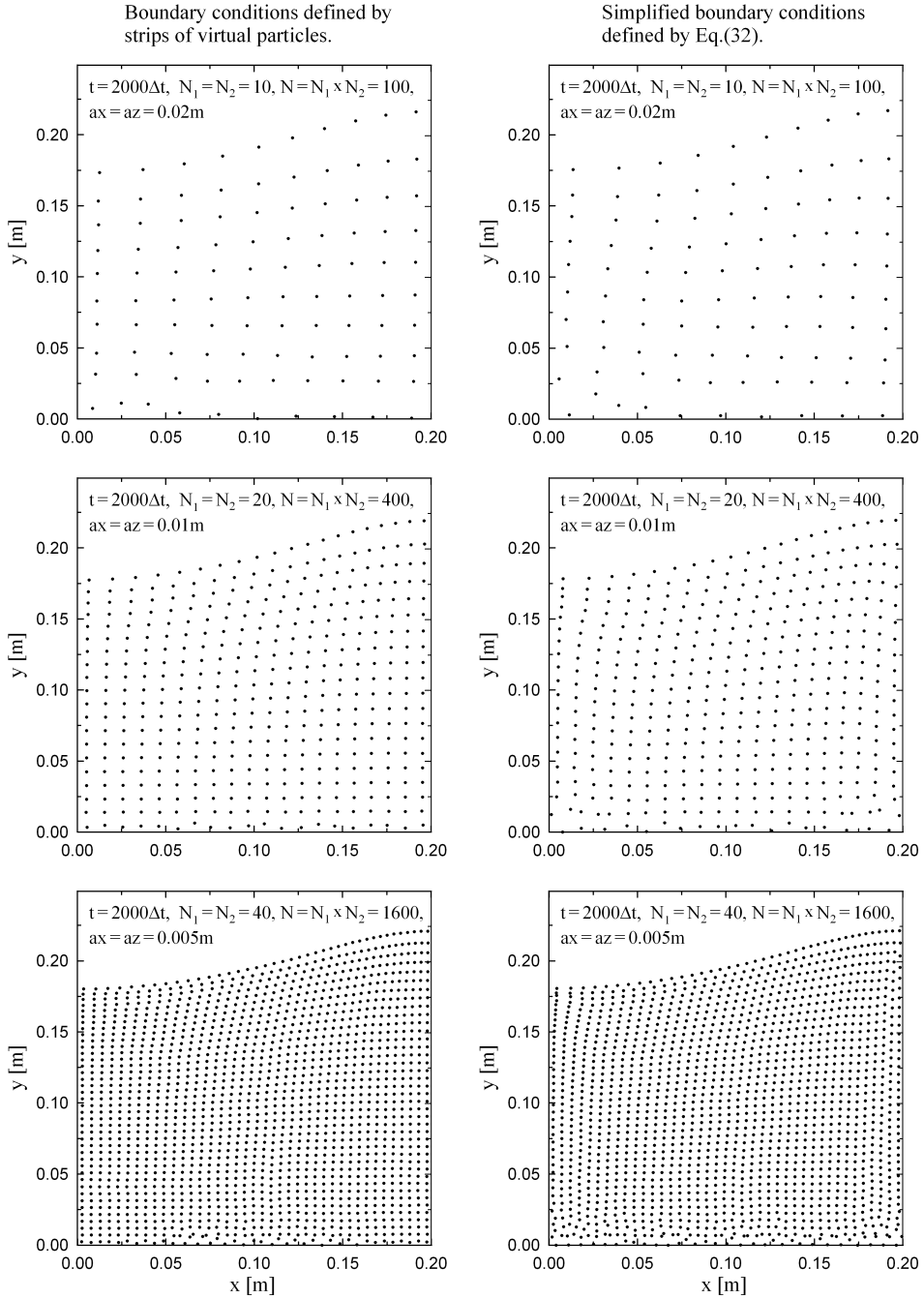


Fig. 5. Continued

particles at selected points in time. The results presented in the figure show that the correction leads to unphysical changes in the fluid density, which confirms our earlier conclusion that the kernel correction is not a proper way to improve the accuracy of calculations. Therefore, in our further calculations, the standard kernel functions, without any correction, were employed.

In order to illustrate the influence of the assumed grid resolution on the SPH results, the three cases of initial inter-particle spacing were considered, which corresponded to the total number of material particles representing the fluid domain  $N = 100$  (400, 1600). The plots in Fig. 4 show the distribution of these particles at selected points in time. Finally, numerical solutions were performed for two formulations of boundary conditions at the solid boundaries of the fluid domain. As mentioned above, the first formulation is based on the mirror reflection of particles within an assumed strip along the boundary, and the second formulation is based on condition equation (32). The numerical results obtained are shown in Fig. 5, in which the plots describe the distribution of particles obtained for the two formulations of boundary conditions. From the graphs, it may be seen that the approximate solution given by equations (32) leads to a distribution with disturbances in the area of the solid boundary that grow in time, especially in the vicinity of the corner points. The overall feature of the solution is preserved, but its accuracy suffers from smaller support domains for particles within areas close to the solid boundary.

## 6. Concluding Remarks

The paper presents a discussion on the approximation aspects of the SPH approach to describing the water wave phenomenon. The main attention has been focused on the reproducing conditions of the SPH formulation. From the continuous integral interpolation, developed in this paper, it follows that an exact reproduction of a given function by means of an integral representation with a positive symmetric kernel is possible only for a linear function (a bilinear function in the two-dimensional case discussed here), for which the second and higher order space derivatives disappear within a solution domain. At the same time, a correction of the kernel functions by means of a linear combination of standard kernels is not unique, and therefore not recommended for describing the water wave phenomenon. From the discussion presented above, it follows that in cases of a relatively regular distribution of fluid particles in space, the correction gives satisfactory results due to the regular distribution. In a general case, however, such a correction may lead to improper solutions from the physical point of view. The example given above illustrates such a case, in which the kernel correction changes the fluid density significantly. The numerical experiments show that the formulation of the boundary conditions, proposed in section (4) of this paper, leads to satisfactory results in the fluid domain, except for the solid boundary areas, in which a certain deterioration of numerical results occurs.

## References

- Ataie-Ashtiani B., Shobeyri and Farhadi L. (2008) Modified incompressible SPH method for simulating free surface problems, *Fluid Dynamics Research*, **40**, 637–661.
- Belytschko T., Krongauz Y., Dolbow J. and Gerlach C. (1998) On the completeness of meshfree particle methods, *Inter. J. for Numerical Methods in Engineering*, **43**, 785–819.
- Bonet J. and Lok T.-S. L. (1999) Variational and momentum preservation aspects of Smooth Particle Hydrodynamic formulations, *Comp. Methods in Appl. Mech. Engrg.*, **180**, 97–115.
- Colagrossi A. and Landrini M. (2003) Numerical simulation of interfacial flows by smoothed particle hydrodynamics, *J. Comp. Phys.*, **191** (2), 448–475.
- Dalrymple R. A. and Rogers B. D. (2006) Numerical modeling of water waves with the SPH Method, *Coastal Engineering*, **53**, 141–147.
- Liu G. R. and Liu M. B. (2009) *Smoothed Particle Hydrodynamics: A Mesh-free Particle Method*, World Scientific, Singapore.
- Lo E. Y. M. and Shao S. (2002) Simulation of near-shore solitary wave mechanics by an incompressible SPH method, *Applied Ocean Research*, **24**, 275–286.
- Monaghan J. J. (1992) Smoothed Particle Hydrodynamics, *Annual Rev. Astrophysics*, **30**, 543–574.
- Monaghan J. J. (2005) Smoothed Particle Hydrodynamics, *Reports on Progress in Physics*, **68**, 1703–1759.
- Monaghan J. J. and Kajtar J. B. (2009) SPH particle boundary forces for arbitrary boundaries, *Computer Physics Communications*, **180**, 1811–1820.
- Morris J. P., Fox P. J. and Zhu Y. (1997) Modeling Low Reynolds Number Incompressible Flows Using SPH, *J. Computational Physics*, **136**, 214–226.
- Staroszczyk R. (2010) Simulation of Dam-Break Flow by a Corrected Smoothed Particle Hydrodynamics Method, *Archives of Hydro-Engineering and Environmental Mechanics*, **57** (1). 61–79.
- Toro E. F. (1997) *Riemann Solvers and Numerical Methods for Fluid Dynamics*, Springer – Verlag, Berlin, Heidelberg.